Semiempirical theory of level spacing distribution beyond the Berry–Robnik regime: modeling the localization and the tunneling effects

2010 J. Phys. A: Math. Theor. 43 215101

(http://iopscience.iop.org/1751-8121/43/21/215101)

IOP PUBLISHING JOURNAL OF PHYSICS A: MATHEMATICAL AND THEORETICAL

J. Phys. A: Math. Theor. **43** (2010) 215101 (28pp) doi:10.1088/1751-8113/43/21/215101

Semiempirical theory of level spacing distribution beyond the Berry–Robnik regime: modeling the localization and the tunneling effects

Benjamin Batistić and Marko Robnik

CAMTP—Center for Applied Mathematics and Theoretical Physics, University of Maribor, Krekova 2, SI-2000 Maribor, Slovenia

E-mail: Benjamin.Batistic@gmail.com and Robnik@uni-mb.si

Received 4 February 2010, in final form 25 March 2010
Published 4 May 2010
Online at stacks.iop.org/JPhysA/43/215101

Abstract

In this work we study the level spacing distribution in the classically mixed-type quantum systems (which are generic), exhibiting regular motion on invariant tori for some initial conditions and chaotic motion for the complementary initial conditions. In the asymptotic regime of the sufficiently deep semiclassical limit (sufficiently small effective Planck constant) the Berry and Robnik (1984 *J. Phys. A: Math. Gen.* **17** 2413) picture applies, which is very well established. We present a new quasi-universal semiempirical theory of the level spacing distribution in a regime away from the Berry–Robnik regime (the near semiclassical limit), by describing both the dynamical localization effects of chaotic eigenstates, and the tunneling effects which couple regular and chaotic eigenstates. The theory works extremely well in the 2D mixed-type billiard system introduced by Robnik (1983 *J. Phys. A: Math. Gen.* **16** 3971) and is also tested in other systems (mushroom billiard and Prosen billiard).

PACS numbers: 01.55.+b, 02.50.Cw, 02.60.Cb, 05.45.Pq, 05.45.Mt, 47.52.+j

(Some figures in this article are in colour only in the electronic version)

1. Introduction

Quantum chaos research of the stationary Schrödinger equation concerns the energy spectra, the eigenfunctions and the matrix elements of other observables (operators) [1–3]. One of the most fundamental findings in quantum chaos was the discovery that the spectral fluctuations (the fluctuations of the spectral staircase function around its smooth average energy level density, after the unfolding, that is after reducing the mean energy level density to 1 everywhere) obey the predictions of the random matrix theory (RMT) [4, 5] if the classical dynamics of the underlying Hamilton system is chaotic (and ergodic). If we do not consider

spin, the existence of the antiunitary symmetries of the system warrants the applicability of the Gaussian orthogonal ensemble (GOE) of random matrices, and of the Gaussian unitary ensemble (GUE) otherwise, where the role of the antiunitary symmetries (the analog of the classical anticanonical symmetries) is non-trivial and important [6, 7]. (In this paper we shall further consider only the systems with an antiunitary symmetry, which includes the GOE case but not GUE.) This so-called Bohigas–Giannoni–Schmit conjecture [8], also initiated by the pioneering ideas of Casati, Valz-Gries and Guarneri [9], has been strongly corroborated by the semiclassical method (Gutzwiller trace formula [1, 2]) and by the results of the spectral autocorrelation function and its Fourier transform (the so-called form factor) first by Berry [10] using the diagonal approximations in evaluating the double sums over classical periodic orbits, and by numerous numerical studies. See e.g. [1, 2, 5]. Relatively recently [11] the leading semiclassical term of the form factor has been supplemented by the next term arising due to the existing pairs of almost identical one-encounter classical unstable periodic orbits in classically ergodic systems with an anticanonical symmetry (such as the time reversal symmetry). This program and procedure have been very recently further developed by Haake's group in Essen [12–14], yielding the final result in complete agreement with the prediction of the RMT to all orders for times shorter than the Heisenberg time, and even for longer times very recently [15]. This implies that e.g. the delta statistics as evaluated in the RMT is completely reproduced by this semiclassical theory. Unfortunately, the most popular statistical spectral measure, the level spacing distribution, depends not only on the two-point spectral correlation function but on all n-point correlation functions.

In the case of completely integrable systems the spectral statistics is Poissonian. This is known since the semiclassical work by Berry and Tabor and is quite obvious (in systems with two or more degrees of freedom). For details, careful numerical calculations and the relevant references see [16]. We also have a kind of a probability limit theorem, stating that a statistically independent superposition of Poissonian number sequences (like the regular eigenenergy spectral sequences are) results again in a Poissonian sequence. Moreover, if we superpose an infinite number of *entirely arbitrary* number sequences with nonvanishing weights we get the Poissonian sequence. Therefore, all the Poissonian level sequences can be lumped together into one single Poissonian sequence.

In the Hamilton systems with classically mixed-type dynamics, which is the generic case, we have classically regular quasi-periodic motion on d-dimensional invariant tori (d is the number of freedoms) for some initial conditions (with the fractional Liouville volume ρ_1) and chaotic motion for the complementary initial conditions (with the fractional Liouville volume $\rho_2 = 1 - \rho_1$). The chaotic set might be further decomposed into several chaotic regions (invariant components) in the case $d = 2$, whilst for $d > 2$ it is strictly speaking always just one chaotic set due to the Arnold diffusion on the Arnold web, which pervades the entire phase space. In a sufficiently deep semiclassical limit the Berry–Robnik (BR) picture [17] is established, based on the statistically independent superposition of the regular (Poissonian) and chaotic level sequences. It was implicitly based on the broad statement of the principle of uniform semiclassical condensation (PUSC) of the Wigner functions of the eigenstates (see [3] and the references therein), which generalizes Berry's assumption of the semiclassical wave functions [18].

Like usual, in this paper we shall consider only the case of just one chaotic component, although the results can be easily generalized for more than one chaotic component. This picture gives an excellent approximation for the statistics of spectral fluctuations of the mixed-type systems, if the largest chaotic component is much larger than the next largest one, which typically indeed is the case e.g. in 2D billiards.

In such a case the energy spectrum of the mixed-type system can be described in the BR regime of a sufficiently small effective Planck constant $\hbar_{\mathrm{eff}}$ by the following formula for the gap probability $E(S)$:

$$E(S) = E_{\mathrm{r}}(\rho_1 S) E_{\mathrm{c}}(\rho_2 S), \tag{1}$$

and the level spacing distribution $P(S)$ (see e.g. [3]) is of course always given as the second derivative of the gap probability, namely $P(S) = \mathrm{d}^2 E(S)/\mathrm{d}S^2$, so that we have

$$P(S) = \frac{\mathrm{d}^2}{\mathrm{d}S^2} E_{\mathrm{r}}(\rho_1 S) E_{\mathrm{c}}(\rho_2 S) = \frac{\mathrm{d}^2 E_{\mathrm{r}}}{\mathrm{d}S^2} E_{\mathrm{c}} + 2\frac{\mathrm{d}E_{\mathrm{r}}}{\mathrm{d}S}\frac{\mathrm{d}E_{\mathrm{c}}}{\mathrm{d}S} + E_{\mathrm{r}}\frac{\mathrm{d}^2 E_{\mathrm{c}}}{\mathrm{d}S^2}. \tag{2}$$

The above factorization formula (1) is a direct consequence of the statistical independence, justified by PUSC. Here by $E_{\mathrm{r}}(S) = \exp(-S)$ we denote the gap probability for the Poissonian sequence with the mean level density 1. By $E_{\mathrm{c}}(S)$ we denote the gap probability for the chaotic level sequence with the mean level density (and spacing) 1. Note that the classical parameter ρ_1 and its complement $\rho_2 = 1 - \rho_1$ enter the expression as weights in the arguments of the gap probabilities.

Using the Bohigas–Giannoni–Schmit conjecture we conclude that in a sufficiently deep semiclassical limit $E_{\mathrm{c}}(S)$ is given by the RMT, and can be well approximated by the Wigner surmise

$$P_W(S) = \frac{\pi S}{2}\exp\left(-\frac{\pi S^2}{4}\right), \qquad F_W(S) = 1 - W_W(S) = \exp\left(-\frac{\pi S^2}{4}\right), \tag{3}$$

such that $E_{\mathrm{c}}(S)$ is equal to

$$E_W(S) = 1 - \mathrm{erf}\left(\frac{\sqrt{\pi}S}{2}\right) = \mathrm{erfc}\left(\frac{\sqrt{\pi}S}{2}\right), \tag{4}$$

where $\mathrm{erf}(x) = \frac{2}{\sqrt{\pi}}\int_0^x \mathrm{e}^{-u^2}\,\mathrm{d}u$ is the error integral and $\mathrm{erfc}(x)$ is its complement, i.e. $\mathrm{erfc}(x) = 1 - \mathrm{erf}(x)$. In equation (3) $W_W(S)$ denotes the cumulative Wigner level spacing distribution $W_W(S) = \int_0^S P_W(x)\,\mathrm{d}x$ and F_W its complement. Under such an assumption the explicit BR formula (in the special case of one regular and one chaotic component) follows immediately:

$$P_{\mathrm{BR}}(S) = \mathrm{e}^{-\rho_1 S}\left\{\mathrm{e}^{-\frac{\pi\rho_2^2 S^2}{4}}\left(2\rho_1\rho_2 + \frac{\pi\rho_2^3 S}{2}\right) + \rho_1^2\,\mathrm{erfc}\left(\frac{\sqrt{\pi}\rho_2 S}{2}\right)\right\}. \tag{5}$$

The correctness of this distribution function in the BR regime (sufficiently small $\hbar_{\mathrm{eff}}$) is by now very well established in highly accurate numerical calculations for all $E(k, L)$ probabilities, not only the gap probability [19].

In the present work the above basic BR formula (1) is generalized in two aspects, in order to describe the main effects of deviation from the BR regime.

First, at not sufficiently small $\hbar_{\mathrm{eff}}$ (e.g. in billiards this means at low energies) the tunneling effects mean overlapping of regular and chaotic eigenfunctions in the classically forbidden region, giving rise to the 'interaction' and level repulsion between the semiclassical regular and chaotic approximate eigenstates, and this coupling can be modeled by dropping the factorization property (1). The couplings can be described in terms of the random matrix ensembles having the BR distribution on the diagonal. Namely, we have the regular, Poissonian, block (denoted by r) of relative size ρ_1 and the chaotic diagonal block (denoted by c) of relative size $\rho_2 = 1 - \rho_1$. The tunneling coupling matrix elements reside only in the off-diagonal blocks coupling the r and c diagonal blocks. The underlying ensemble of such block random matrices has been introduced and termed TDBR ensemble (tunneling distorted Berry–Robnik) in a recent work by Vidmar *et al* [20]. An essentially 2D (two-level) analytic

model has been derived there. It will be shown in the present work that this analytic model is very successful at all spacings, whilst the TDBR ensemble of large matrices itself does not correctly capture the behavior of real (billiard) spectra at small spacings, and an alternative random matrix model, tunneling distorted Berry–Robnik–Brody (TBRB), will be introduced, which is correctly described by the said analytic coupling model of Vidmar *et al* [20]. As for the coupling matrix elements in this context, we should note that it is natural, but not absolutely necessary, to assume the Gaussian distribution for the coupling matrix elements, with zero mean and the variance σ^2. The results depend only weakly on the kind of the distribution functions as long as they have the same variance σ^2.

Second, at not sufficiently small $\hbar_{\mathrm{eff}}$ (e.g. in billiards this means at low energies) the chaotic eigenstates (their Wigner functions in the phase space) are not uniformly extended over the entire classically allowed chaotic component, but are localized, i.e. effectively occupying a volume smaller than the volume ρ_2 of the entire classically chaotic component, the reason being the dynamical localization effect (see e.g. the excellent review paper by Prosen [21] and the references therein), discovered and explained by Chirikov, Casati, Izrailev, Shepelyanski and Guarneri around the 1980s. (For a general overview see also [1, 2].) In the context of the time-dependent Floquet systems, such as the kicked rotator, the dynamical localization has been very extensively studied. For a review, see e.g. the paper by Izrailev [22]. It has been observed that in parallel with the localization of the eigenstates one observes the fractional power law level repulsion (of the quasi-energies) even in a fully chaotic regime (of the kicked rotator), and it is believed that this picture also applies to time-independent (autonomous) Hamilton systems and their eigenstates. Thus, we see the crossover behavior from GOE in the case of extended chaotic states to the Poissonian statistics in the case of strong localization. The level spacing distribution in such a transition regime of localized but chaotic eigenstates can be described by the well-known Brody distribution with the only one family parameter β:

$$P_{\mathrm{B}}(S) = C_1 S^{\beta} \exp(-C_2 S^{\beta+1}), \qquad F_{\mathrm{B}}(S) = 1 - W_{\mathrm{B}}(S) = \exp(-C_2 S^{\beta+1}), \tag{6}$$

where the two parameters C_1 and C_2 are determined by the two normalizations $\langle 1\rangle = \langle S\rangle = 1$, and are given by

$$C_1 = (\beta+1)C_2, \qquad C_2 = \left(\Gamma\left(\frac{\beta+2}{\beta+1}\right)\right)^{\beta+1}, \tag{7}$$

with $\Gamma(x)$ being the Gamma function. If we have extended chaotic states $\beta = 1$ and RMT (3) applies, whilst in the strongly localized regime $\beta = 0$ and we have Poissonian statistics. Again, by $W_{\mathrm{B}}(S)$ we denote the cumulative Brody level spacing distribution, $W_{\mathrm{B}}(S) = \int_0^S P_{\mathrm{B}}(x)\,\mathrm{d}x$, and by $F_{\mathrm{B}}(S)$ its complement. The corresponding gap probability is

$$E_{\mathrm{B}}(S) = \frac{1}{(\beta+1)\Gamma\left(\frac{\beta+2}{\beta+1}\right)} Q\left(\frac{1}{\beta+1}, \left(\Gamma\left(\frac{\beta+2}{\beta+1}\right) S\right)^{\beta+1}\right), \tag{8}$$

where $Q(\alpha, x)$ is the incomplete Gamma function:

$$Q(\alpha, x) = \int_x^{\infty} t^{\alpha-1}\,\mathrm{e}^{-t}\,\mathrm{d}t. \tag{9}$$

By choosing $E_{\mathrm{c}}(S)$ in equation (1) as given in (8) we are able to describe the localization effects on the chaotic component. Such an approach has already been proposed in the paper by Prosen and Robnik [23, 24], and the resulting level spacing distribution, emerging from this assumption, was called Berry–Robnik–Brody (BRB). It has two parameters: the classical parameter ρ_1 and the quantum parameter β.

It will turn out that this description is indeed excellent, and in addition, where the tunneling effects become important, we combine this ansatz with the coupling picture to be described

in section 2 for random matrix ensembles, like the analytic coupling model in [20] by Vidmar *et al*, yielding then a three-parameter distribution with parameters ρ_1, β and σ, for which we find an excellent analytic description based on 2D matrices. The physical meaning of the three parameters is very clear: ρ_1 characterizes the division of the classical phase space into a regular and chaotic component, β describes the degree of localization of Wigner functions of the chaotic eigenstates on the classically chaotic component and σ measures the strength of the tunneling couplings between the regular and chaotic eigenstates. The latter two parameters must be understood as their average values over the eigenstates within the energy interval that we consider. We call the resulting theory the TBRB theory.

The applicability of the Brody distribution in this context is still not well understood, but we shall see that the theory describes very well the empirical data from the highly accurate energy spectra of billiards at energies around and below the BR regime. Therefore, the resulting theory is of semiempirical nature, but seems to be quasi-universal in the sense that below the BR regime we indeed find spectral fluctuations, in particular the level spacing distribution, which are well described by our theory on the very finest scale of level spacings. We have also tried to use other one-parametric level spacing distributions instead of Brody, like e.g. those proposed and studied in Izrailev's papers [22, 25] (see also [26]), but must definitely conclude that the Brody distribution is quite special; it gives by far the best agreement between the theory and real spectra.

As we shall show, the dynamical localization effects can persist up to very high-lying eigenstates, even up to one million, whilst the tunneling effects occur usually only at very low-lying eigenstates, due to the exponential dependence on the reciprocal effective Planck constant, $\propto \exp(-\text{const}/\hbar_{\text{eff}})$.

The paper is structured as follows: in section 2 we develop the analytical theory based essentially on a two-level approach (2D random matrices), and in section 3 we introduce the corresponding large (high-dimensional) ensembles of random block-structured matrices, and test the accuracy of the analytic theory. In section 4 we present the numerical results for the by far the best investigated billiard [34, 35] with $\lambda = 0.15$, and in section 5 we analyze the numerical spectra for other shapes of the same billiard family. In section 6 we analyze the mushroom billiard introduced by Bunimovich [27] and the Prosen billiard [28, 29]. In section 7, we discuss our results and give the main conclusions.

2. 2D real symmetric random matrices in the spirit of TBRB theory

Consider 2×2 symmetric matrices $A = (A_{ij})$, where $i, j = 1$ or 2. In the present context only the difference between eigenvalues is of relevance. Without loss of generality (see [30]) we may thus assume that the trace of A vanishes, i.e.

$$A = \begin{pmatrix} a & b \\ b & -a \end{pmatrix}, \tag{10}$$

where a and b are real. Introducing the polar coordinates $a = r\cos\varphi, \quad b = r\sin\varphi$, where $r \in [0, \infty)$ and $0 \leqslant \varphi \leqslant 2\pi$, we can derive the general formula [31] for the level spacing distribution:

$$P(S) = \frac{S}{4}\int_0^{2\pi} \mathrm{d}\varphi\, g_a\left(\frac{S}{2}\cos\varphi\right) g_b\left(\frac{S}{2}\sin\varphi\right), \tag{11}$$

where $g_a(a)$ and $g_b(b)$ are the normalized but so far completely arbitrary probability densities for the matrix elements a and b, respectively. By construction the distribution (11) is automatically normalized, $\langle 1\rangle = 1$, but in general this is not true for the first moment,

$\langle S\rangle \neq 1$. If we want to use it as a model distribution for real, experimental, spectra after the spectral unfolding, it must be normalized to the unit mean level spacing $\langle S\rangle = 1$. Such a normalized distribution will be denoted by $P^n(S)$. It can be easily obtained by rescaling the argument of $P(S)$ by a scale factor B:

$$P^n(S) = BP(BS), \qquad \text{with} \qquad B = \int_0^\infty xP(x)\,\mathrm{d}x. \tag{12}$$

If $g_a(x)$ and $g_b(x)$ are regular and non-zero at $x = 0$, then the integrand at $S = 0$ is just a non-zero number equal to $g_a(0)g_b(0)$, and we get for small S

$$P(S) \approx \frac{\pi S}{2} g_a(0)g_b(0). \tag{13}$$

Thus, in the case where both g_a and g_b are regular and non-zero at $S = 0$ we always have linear level repulsion. This linear level repulsion law is very robust, and it depends only on the regularity properties of the distribution functions of the matrix elements at a zero value. For regular distribution functions $g_{a,b}(x)$ higher order corrections in S to this formula can be obtained from Taylor expansions of $g_a(x)$ and $g_b(x)$ around $x = 0$. If either $g_a(x)$ or $g_b(x)$ is zero at $x = 0$, the level repulsion is no longer linear, but of higher order, e.g. quadratic or even cubic, depending on the behavior of $g_a(x)$ and $g_b(x)$ at $x = 0$. We also see that the level repulsion is not linear in S, if $g_a(0)$ and $g_b(0)$ do not exist, since the distributions $g_a(x)$ and $g_b(x)$ are singular at $x = 0$. In such a case we obtain a fractional power law level repulsion discovered and studied in detail in [23, 24, 32, 33]. Indeed, we shall analyze this important case in another paper, following a preliminary study in [31].

In the present paper we shall consider only the cases where the distribution of the off-diagonal elements $g_b(x)$ is Gaussian with the variance σ^2, or exponential, with the same variance. In the former case we have

$$g_b(b) = \frac{1}{\sigma\sqrt{2\pi}} \exp\left(-\frac{b^2}{2\sigma^2}\right), \tag{14}$$

and in the latter case

$$g_b(b) = \frac{\sqrt{2}}{2\sigma} \exp\left(-\frac{|b|\sqrt{2}}{\sigma}\right), \tag{15}$$

where we have assumed that $g_b(b)$ is an even function of b.

We should note that the energy level density (= eigenvalue density) $n(E)$ of our general 2D matrices in (10) with the level spacing distribution (11) is given exactly by the formula

$$n(E) = P(2|E|), \tag{16}$$

where $|E|$ is the absolute value of the eigenvalue E.

Let us now assume that the diagonal distribution $g_a(a)$ is such that when b is forced to be zero $b = 0$ (namely, $g_b(b) = \delta(b)$, $\delta(x)$ being the Dirac delta function), we have a prescribed level spacing distribution $P_0(S)$. Assuming that $g_a(a)$ is also an even function of a, we immediately obtain

$$g_a(a) = P_0(2|a|). \tag{17}$$

First we reconsider the TDBR theory presented in [20]. In order to describe the couplings due to tunneling, it is then natural to consider $g_a(a)$ as derived from the BR level spacing distribution (choosing $P_0(S) = P_{\mathrm{BR}}(S)$, see equation (5)) and then to calculate the tunneling distorted distribution by using the following statistically averaged coupling distribution [20]:

$$g_b(b) = 2\rho_1(1-\rho_1)\frac{1}{\sigma\sqrt{2\pi}} \exp\left(-\frac{b^2}{2\sigma^2}\right) + [1 - 2\rho_1(1-\rho_1)]\delta(b). \tag{18}$$

The resulting analytic theory has been tested in real spectra [20] and good agreement has been found except for the small spacings S.

But we can do much better by going a little bit more deeply into the structure of the basic formulas (1) and (2). So now we proceed to calculate an analytic approximation for TDBR within such a 2D (two-level) random matrix scheme. For $E_c(S)$ we shall assume the Brody formula (8), in order to capture the localization effects on the chaotic component c.

We go back to the fundamental formulas (1) and (2) and write down explicitly the three contributions to the level spacing distribution

$$P(S) = \frac{d^2E_r}{dS^2}E_c + 2\frac{dE_r}{dS}\frac{dE_c}{dS} + E_r\frac{d^2E_c}{dS^2}, \tag{19}$$

where now $E_c(\rho_2 S)$ is the gap probability of the Brody distribution (8), and interpret them as follows.

- $P_{rr}(S) = \frac{d^2E_r}{dS^2}E_c$ is the probability density that two regular levels are separated by a distance S without any regular level in between (the first factor), and also no chaotic level in between (the second factor). The integral $\int_0^\infty P_{rr}(S)\,dS$ is the probability that two nearest neighbors are both regular ones.
- $P_{rc}(S) = 2\frac{dE_r}{dS}\frac{dE_c}{dS}$ is the probability density that the regular and chaotic levels are separated by a distance S without any other level in between. The integral $\int_0^\infty P_{rc}(S)\,dS$ is the probability that two nearest levels are a pair of the chaotic and regular level.
- $P_{cc}(S) = E_r\frac{d^2E_c}{dS^2}$ is the probability density that two chaotic levels are separated by a distance S without any chaotic level in between (the second factor) and also no regular level in between (the first factor). The integral $\int_0^\infty P_{cc}(S)dS$ is the probability that two nearest neighbors are both chaotic ones.

With this insight we can now describe the couplings between the regular and chaotic levels only (i.e. no r–r and no c–c correlations) due to the tunneling. In (11) we assume $P_0(S) = P_{rc}(S)$. According to (17) we have $g_a(a) = P_{rc}(2|a|)$, and we assume the Gaussian couplings (14), leading to *the first central result of this paper:*

$$P(S) = P_{rr}(S) + P_{cc}(S) + \frac{S}{\sigma\sqrt{2\pi}}\int_0^{\pi/2} P_{rc}(S\cos\varphi)\exp\left(-\frac{(S\sin\varphi)^2}{8\sigma^2}\right)d\varphi. \tag{20}$$

(Here we have used the fact that $g_a(a)$ and $g_b(b)$ are even functions of their argument. This formula is also referred to as the improved two-level theory of the generalized TDBR distribution, generalized in the sense that the localization effects are included, and that it corresponds to the block matrices with only c–r couplings included (T-model). See appendix C.) If, instead, we use the exponential couplings (15) rather than Gaussian, but with the same variance σ^2, we find

$$P(S) = P_{rr}(S) + P_{cc}(S) + \frac{S\sqrt{2}}{2\sigma}\int_0^{\pi/2} P_{rc}(S\cos\varphi)\exp\left(-\frac{S\sin\varphi}{\sigma\sqrt{2}}\right)d\varphi. \tag{21}$$

It should be noted that *a priori* there is no universal modeling of the coupling distribution $g_b(b)$, and thus various distributions can be used. But for several reasons the Gaussian couplings are most meaningful. Nevertheless, on several occasions we have tested the dependence of the final results at small σ on the choice of $g_b(b)$ with the same variance σ^2, and found that this dependence is indeed very weak. In the following we shall always assume Gaussian model unless stated otherwise.

The distribution (20) is the sought generalized analytic model of the level spacing distribution of the TDBR random matrix model of [20] with the three parameters ρ_1, β

and σ. It is normalized to a unit total probability, but its first moment is not yet equal to 1. Before using it we must normalize the first moment to 1 as described in equation (12).

In the case $\beta = 1$ this is the improved analytic two-level model of the tunneling coupled random matrices of the TDBR matrix model in [20]. It agrees with the analytical formula (18) derived in [20] only for large S values, and deviates from that at S of the order of few σ. This also becomes clear if we compare the constant and non-zero values of the underlying level spacing distributions at zero level spacing $S = 0$, namely we find:

- For the BR distribution (5): $P(0) = \rho_1(2 - \rho_1)$
- For the coupling model (18) [20]: $P(0) = \rho_1(2 - \rho_1)\big(1 - 2\rho_1 + 2\rho_1^2\big)$
- For the coupling model (20) (with $\beta \neq 0$): $P(0) = \rho_1^2$.

The effect can be graphically clearly seen in figures 4, 5 and 6 of [20]. For the underlying high-dimensional matrix models, TDBR, the actual $P(S)$ goes down to zero as $S \to 0$, which is still not the case in our present improved analytical model, but it comes very close to that. In fact, there is a very small, exponentially small linear regime, where $P(S)$ goes steeply down to zero from the value ρ_1^2.

The improvement of our two-level analytic model of the high-dimensional generalized TDBR matrix ensemble [20] is thus considerable.

However, we have found out empirically that this model along with its best analytical formula (20) is only a good starting approximation. Namely, it turns out, quite surprisingly that the coupling model (18) developed in [20] is a much better description of the real energy spectra of dynamical systems, such as 2D billiards, than formula (20), especially at small values of S.

Therefore, *the second central result of this paper* is that the couplings described in (18) lead to the correct description of real energy spectra, up to the values of order $\sigma \approx 0.1$. The corresponding random matrix ensemble is not the TDBR model in [20], but instead the sparsed random matrix ensemble with uniformly spread non-zero off-diagonal Gaussian distributed matrix elements (14) (sparsed all-to-all couplings) with the sparsity parameter $s = 2\rho_1\rho_2 = 2\rho_1(1 - \rho_1)$ (s is the fraction of the non-zero off-diagonal matrix elements).

The physical explanation of this finding is still open, but certainly relates to the fact that not each regular level is coupled to each chaotic level, but instead these couplings depend on the energy closeness and geometrical closeness of the eigenstates and corresponding semiclassical Wigner functions. Thus to explain it we must study the quantum mechanics in the phase space, that is the Wigner functions, in more detail. This is open in our future research. However, we have a heuristic argument. In appendix C we show the two relevant random matrix coupling models, the T-model (TDBR) and the S-model (TBRB). We assume that in the case of clear separation of the regular and chaotic basis states the T-model is the correct description of the spectral correlations. But if we do not know anything about the mixed-type Hamilton system, but only the fact that the diagonal matrix elements have the BRB level spacing distribution, then we must allow for a *random* permutation of the diagonal elements, or—keeping the diagonal block structure—we assume randomly and uniformly distributed non-zero (Gaussian) coupling matrix elements, then obviously with the sparsity parameter $s = 2N_rN_c/(N^2 - N) = 2N^2\rho_1\rho_2/(N^2 - N) \approx 2\rho_1\rho_2$, which is then the S-model.

To conclude this section, we propose that the correct semiempirical theory of the regime just below the BR regime in real quantal energy spectra is the generalized Berry–Robnik–Brody theory which we shall call TBRB theory, corresponding to the S-model.

The special case without couplings, describing the dynamical localization effects, reduces precisely to the BRB theory devised by Prosen and Robnik [23, 24]. The resulting level

spacing distribution $P_{\mathrm{BRB}}(S)$ is derived from (2) with $E_{\mathrm{r}}(S) = \exp(-S)$ being Poissonian gap probability, and $E_{\mathrm{c}}(S) = E_{\mathrm{B}}(S)$, as given in equation (8), being the Brody gap probability with a given parameter β measuring the degree of (dynamical) localization.

If there are couplings due to the tunnelings, which is the general case, we find semiempirically that the correct level spacing distribution is described by the coupling formula (11) with $g_a(a) = P_{\mathrm{BRB}}(2|a|)$ and $g_b(b)$ in (18) as introduced in [20], and $P_{\mathrm{BRB}}(S)$ denotes the Berry–Robnik–Brody level spacing distribution described above.

Therefore, *the second central result of this paper* can be summarized in the final formula, like in (11), namely

$$P(S) = \frac{2\rho_1(1-\rho_1)S}{\sigma\sqrt{2\pi}} \int_0^{\pi/2} P_{\mathrm{BRB}}(S\cos\varphi) \exp\left(-\frac{(S\sin\varphi)^2}{8\sigma^2}\right) \mathrm{d}\varphi + (1 - 2\rho_1(1-\rho_1))\, P_{\mathrm{BRB}}(S), \tag{22}$$

where $P_{\mathrm{BRB}}(S)$ is the Berry–Robnik–Brody level spacing distribution derived from (1), (2) and (6)–(8). In appendix C we give an overview of the three random matrix models and the corresponding two-level coupling theory.

3. Numerical studies of the analytical models and the corresponding ensembles of large matrices: TDBR and TBRB

The quality and validity of our analytic theory (20) should be first tested for the N dimensional random matrix ensembles generalizing (10).

We assume on the diagonal a Poissonian block of relative size ρ_1, followed by a chaotic block of relative size $\rho_2 = 1 - \rho_1$ obeying the Brody distribution (6) and (8) with a given β, and for the off-diagonal block coupling only r and c levels we assume precisely the Gaussian distribution (14). This is precisely the generalized TDBR random matrix model, generalized in the sense that in general $0 \leqslant \beta \leqslant 1$, describing the localization effects, whilst in [20] $\beta = 1$. In appendix C this is the T-model.

Numerical calculations have been performed using such an ensemble of matrices of size $N = 4000$. To avoid the finite size effects we have used in the statistical analysis only the middle 2000 levels, and drew from the ensemble 1000 matrices. The unavoidable problem with some ambiguity and arbitrariness of the spectral unfolding has been treated by using the most preferred global empirical unfolding using the average over the entire spectral stretch. This is very important, as we found a very strong dependence of the results upon the choice of the local unfolding (average over a certain number γ of neighbors), and only in the case of the global unfolding the results agree with the analytical theory.

When comparing the numerical results with our analytic theory (20) on the largest scale in the standard representation $P(S)$ versus S, we saw within the graphical resolution no deviations between the numerical experiment and the theory. Therefore, in order to exhibit the finest details of the excellent agreement between the theory and the numerics we use the so-called U-function representation, which is the following transcendental transformation of the cumulative (or integrated) level spacing distribution $W(S) = \int_0^S P(x)\,\mathrm{d}x$, introduced by Prosen and Robnik in [24]:

$$U(S) = \frac{2}{\pi} \arccos\sqrt{1 - W(S)}. \tag{23}$$

The U-function has the advantage that its expected statistical error δU is independent of S, it is constant for all S and equal to

$$\delta U = \frac{1}{\pi\sqrt{N_s}}, \tag{24}$$

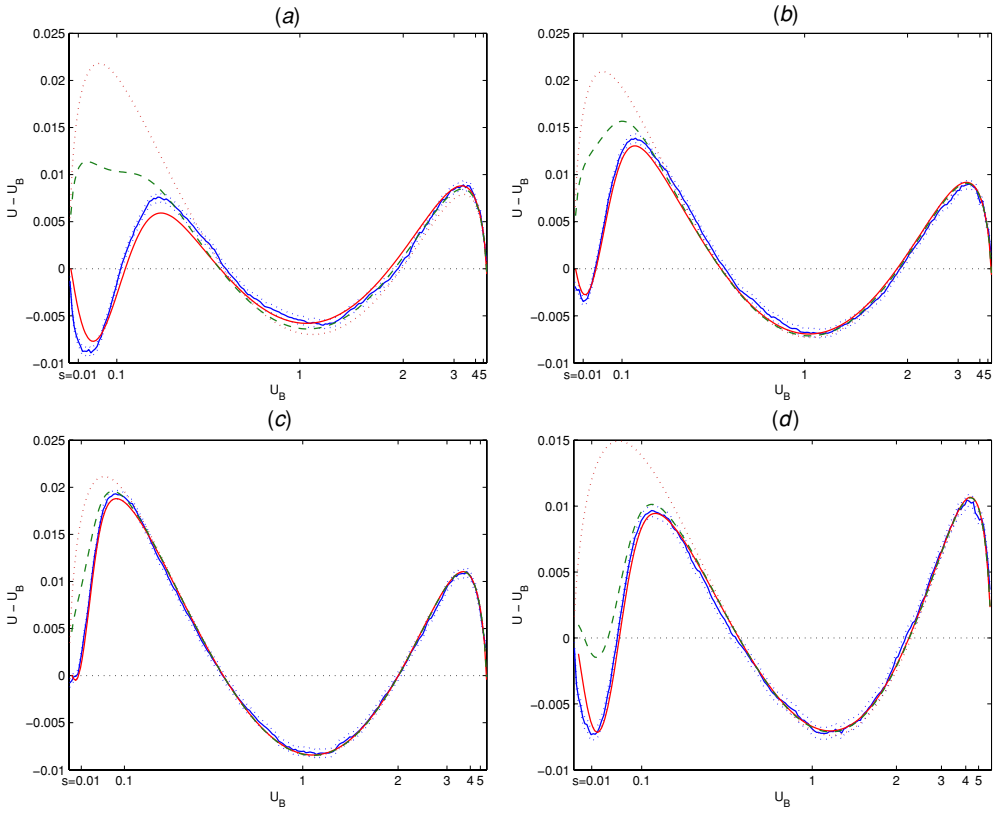

Figure 1. $U - U_{\rm B}$ versus $U_{\rm B}$ and nonlinear scale of S for the generalized 2D TDBR theory (full line) and large generalized TDBR matrices (the numerical data with $\pm$ standard deviation strip), the TBRB curve (dashed) (couplings like in Vidmar *et al* [20]) and (dotted) BRB curve ($\sigma = 0$). The parameter values are: ($\rho_1 = 0.2,\ \beta = 0.7,\ \sigma = 0.05$) (*a*), ($\rho_1 = 0.2,\ \beta = 0.7,\ \sigma = 0.025$) (*b*), ($\rho_1 = 0.3,\ \beta = 0.7,\ \sigma = 0.01$) (*c*) and ($\rho_1 = 0.5,\ \beta = 0.7,\ \sigma = 0.02$) (*d*). The analytical 2D TDBR formula is evidently excellent approximation for large generalized TDBR matrices.

where N_s is the total number of objects in the $W(S)$ distribution. The constant prefactor in (23) is chosen such that $U(S)$ goes from 0 to 1 when $W(S)$ goes from 0 to 1. For the completeness of our exposition, we give a short derivation in appendix A.

In figure 1(*a*) we plot our results for the particular case $\rho_1 = 0.2$, $\beta = 0.7$ and $\sigma = 0.05$. We plot not the U-function itself, but the fine difference $U(S) - U_{\rm B}(S)$, where $U_{\rm B}$ is the U-function of the Brody distribution that is

$$U_{\rm B}(S) = \frac{2}{\pi} \arccos \sqrt{1 - W_{\rm B}(S)}, \tag{25}$$

where the Brody cumulative level spacing distribution $W_{\rm B}(S)$ is given by equation (6). We plot this difference not versus S but instead versus $U_{\rm B}$, and indicate on the abscissa the nonlinear scale of S. If the Brody distribution itself were a perfect description of data, the curve would lie on the abscissa. The fact that we have nonvanishing ρ_1 and couplings of 'strength' $\sigma = 0.05$ implies expected deviation from the abscissa (Brody). We show the strip of the numerical data of $U(S)$ with the indicated $\pm\delta U$ error for the matrices, and also the theoretical curve (no fitting!) from our two-level theory (20). The agreement is really perfect.

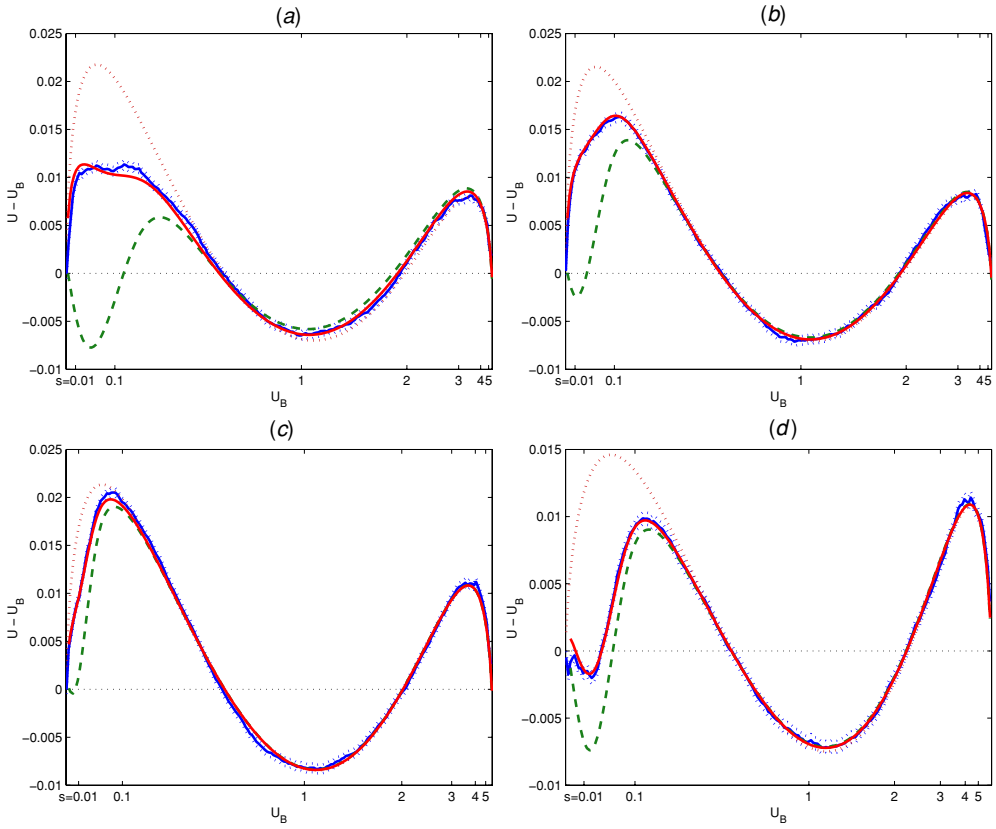

Figure 2. $U - U_{\rm B}$ versus $U_{\rm B}$ and nonlinear scale of S for the 2D TBRB theory (full line) and large TBRB matrices (the numerical data with $\pm$ standard deviation strip), the generalized TDBR curve (dashed) and (dotted) BRB curve ($\sigma = 0$). The parameter values are: ($\rho_1 = 0.2,\ \beta = 0.7,\ \sigma = 0.05$) (*a*), ($\rho_1 = 0.2,\ \beta = 0.7,\ \sigma = 0.025$) (*b*), ($\rho_1 = 0.3,\ \beta = 0.7,\ \sigma = 0.01$) (*c*) and ($\rho_1 = 0.5,\ \beta = 0.7,\ \sigma = 0.02$) (*d*). The analytical 2D TBRB formula is evidently excellent approximation for large generalized TBRB matrices.

Moreover, we show that the theory based on the coupling assumption (18) used in the previous work by Vidmar *et al* [20] (dashed curve), and now generalized to the TBRB theory, follows the numerical data only for large $S > 0.3$, and then deviates greatly from the present theory at smaller S. It is this latter theory, TBRB, which correctly captures the spectral properties of real spectra, as will be shown in the next section. In appendix C this is the S-model.

In figures 1(*b*)–(*d*) we show three more cases at smaller σ demonstrating that the agreement with the generalized TDBR theory (20) is perfect, namely for the parameter values ($\rho_1 = 0.2,\ \beta = 0.7,\ \sigma = 0.025$), ($\rho_1 = 0.3,\ \beta = 0.7,\ \sigma = 0.01$) and ($\rho_1 = 0.5,\ \beta = 0.7,\ \sigma = 0.02$), respectively.

In figures 2(*a*)–(*d*) we show analogous plots for the analytic 2D TBRB theory in comparison with the corresponding large matrix ensembles introduced in section 2, where we have a BRB diagonal block, with the uniformly randomly spread non-zero off-diagonal matrix elements, having the Gaussian distribution with a given variance σ^2 and the sparsity parameter $s = 2\rho_1\rho_2 = 2\rho_1(1 - \rho_1)$. The dimensions of the matrices and the procedure

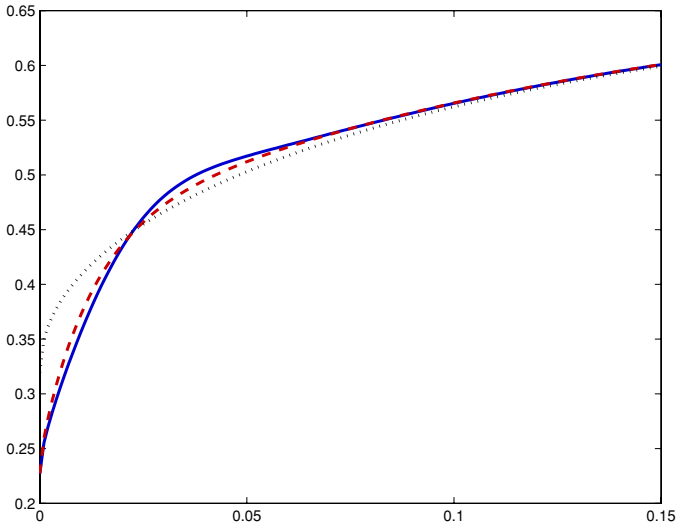

Figure 3. Gaussian (full) and exponential (dashed) TBRB $P(S)$ versus S for $\rho_1 = 0.175$, $\beta = 0.47$ and $\sigma = 0.01$, for $0 < S < 0.35$. The dotted curve is for $\sigma = 0$.

of calculating their level spacing distribution are exactly the same as in figure 1. Excellent agreement of the TBRB theory and the numerics is found (there is no fitting here!).

Finally, we should mention that switching from the model with Gaussian couplings (14) to the exponential couplings (15) in equation (22) at such a small $\sigma = 0.01$ makes a small difference in $P(S)$ as shown in figure 3, confirming the expectation that it is the variance σ^2 which matters in this respect but not the details of the distribution of the coupling matrix elements $g_b(b)$. Note that the two curves coincide for $S > 0.1$.

At the larger value of $\sigma = 0.05$ we see larger deviations, but still not very dramatic, in figure 4. Note that the two curves coincide for $S > 0.3$. Probably we can conclude that the Gaussian model of the couplings is the most natural one, and emerges naturally as a result of certain averaging of the couplings over a large number of eigenstates in the energy interval that we consider in dynamical systems.

4. Numerical spectra in a 2D mixed-type billiard and application of the BRB theory

After setting up our analytic theory (TBRB), resulting in formula (22), and comparing it with the generalized TDBR ensembles of random matrices of the type 'BRB diagonal + off-diagonal *r-c* tunneling couplings', as described in section 3, we proceed by applying the TBRB theory in real dynamical systems. It will be seen that in most systems the tunneling couplings are practically absent—except at very small energies—due to the exponential dependence on $1/\hbar_{\mathrm{eff}}$. On the other hand the effects of dynamical localization persist up to very high-lying eigenstates, sometimes even up to one million above the ground state. In this and in the next section we shall see examples, billiard models, in which tunneling effects are completely absent, that is $\sigma = 0$. This is then just the BRB theory as a special case of TBRB.

We have chosen the one parameter family of 2D billiards introduced and studied first classically in [34], and quantally in [35]. The billiard boundary is defined in the physical complex w plane as the quadratic conformal map $w(z) = z + \lambda z^2$ of the unit circle $|z| = 1$ in

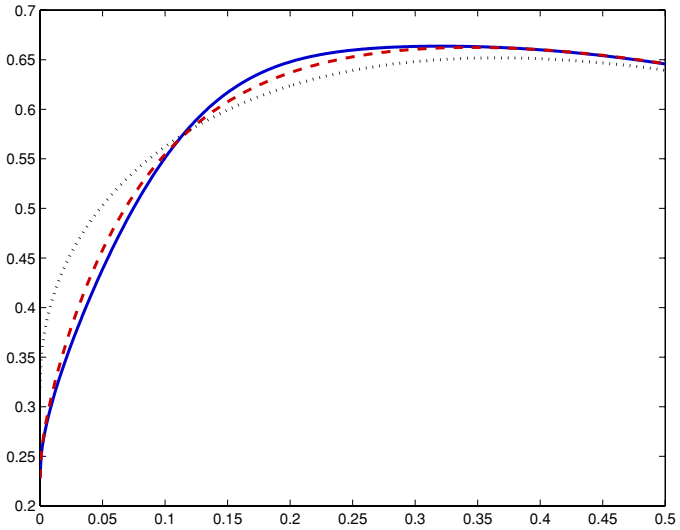

Figure 4. Gaussian (full) and exponential (dashed) TBRB $P(S)$ versus S for $\rho_1 = 0.175$, $\beta = 0.47$ and $\sigma = 0.05$, for $0 < S < 0.5$. The dotted curve is for $\sigma = 0$.

the complex z-plane. We have used a variety of different shapes λ equal to 0.125, 0.14, 0.15, 0.16, 0.175, 0.20 and 0.25. The corresponding classical parameter ρ_1 has been very carefully and accurately calculated using the method based on [36], with the values (accurate better than within 1%), respectively: 0.38, 0.24, 0.175, 0.121, 0.05, 0.0 and 0.0. The details of the method and the tests are given in appendix B.

The energy spectra have been calculated with great accuracy, much better than 1% of the mean level spacing; we estimated the largest error as smaller than 0.3% of the mean level spacing. First we used the basic method of the conformal mapping diagonalization technique proposed and used in [35], and improved in [32], yielding about 50 000 lowest levels within the above mentioned accuracy. The accuracy was cross-checked with yet another almost general method published in [37], the so-called expanded boundary integral method, and perfect agreement was found. For higher levels we had to stick to another method, namely the scaling method of Vergini and Saraceno [38], in two versions, the first based on plane waves and the second on circular waves. Perfect agreement was achieved. In order to go to even higher energies we had to employ the singular value decomposition methods to find sufficiently accurate results when dealing with the large and almost singular matrices. Therefore, after accomplishing these techniques, we have complete confidence in the above-stated accuracy of our numerical energy spectra of the billiard.

As for the unfolding procedure we have used strictly and exclusively the exact Weyl formula with perimeter and curvature corrections. Namely, if the Helmholtz equation in our units is written as $\Delta\psi + E\psi = 0$, then the Weyl formula for the number of energy levels up to the energy E reads $\mathcal{N}(E) = \mathcal{A}E/(4\pi) - \mathcal{L}\sqrt{E}/(4\pi) + 1/6$, where $\mathcal{A}$ and $\mathcal{L}$ are the area and the perimeter of the billiard, respectively, and we assume the Dirichlet boundary conditions.

When analyzing the small effects that we are studying in the level spacing distribution for the large matrices from the TBRB ensemble we found that they are very sensitively dependent on the choice of an empirical unfolding procedure, which usually means taking a local average of the level spacings up and down in the spectrum by a certain number of γ neighbours.

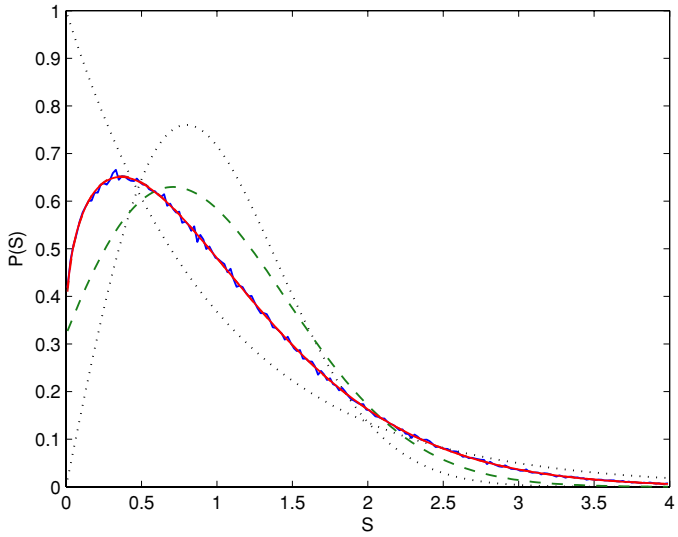

Figure 5. The level spacing distribution for the billiard $\lambda = 0.15$, compared with the analytical formula for 2D TBRB (full line) with parameter values $\rho_1 = 0.183$, $\beta = 0.465$ and $\sigma = 0$. The dashed curve close to the full line is TBRB with classical $\rho_1 = 0.175$ is not visible, as it overlaps completely with the quantum case $\rho_1 = 0.183$. The dashed curve far away from the full line is just the BR curve with the classical $\rho_1 = 0.175$. The Poisson and GOE curves (dotted) are shown for comparison. The agreement of the numerical spectra with TBRB at $\sigma = 0$ (which is just BRB) is perfect. In the histogram we have 650 000 objects; therefore, the statistical significance is extremely large.

Changing γ has drastically changed the structure of the U-function plots introduced in the previous section, overshadowing the physical effects. We should mention that, nevertheless, in the usual large scale representation $P(S)$ (P versus S) these effects were entirely invisible within the graphical resolution.

For the sake of analyzing the real billiard spectra, we have thus completely abandoned using the ensembles of large matrices, due to the ambiguity of the unfolding procedure. Therefore, we have compared the results of the numerical billiard energy spectra only to our analytic TBRB theory developed in section 2, thereby completely avoiding the numerical unfolding procedures in large matrices.

Our best example and most extensively studied case $\lambda = 0.15$ is shown in figure 5 for the standard representation $P(S)$. The parameters are $\rho_1 = 0.175$, $\beta = 0.465$ and $\sigma = 0$. On this scale we have just perfect agreement between the numerical data and the TBRB theory.

To see the effects more clearly a much more sensitive representation is necessary. This is shown in figure 6 where we present the decadic log–log plot of $\log W(S) - \log W_{\mathrm{B}}(\mathrm{S})$, versus $\log S$, where $W_{\mathrm{B}}(\mathrm{S})$ is the best fitting Brody distribution with $\beta = 0.313$, obtained over the interval $0.001 \leqslant S \leqslant 1$. The best fitting BRB distribution (the full line) has $\beta = 0.465$. We see that BRB model is indeed highly accurate, as it captures the data over the interval $S \in (0.0001, 1)$, on the interval $S \in (0.001, 1)$ even excellently, and the fluctuations at $S \leqslant 0.001$ are probably of purely statistical nature. We could say that the fractional power law level behavior (straight line) is observed roughly on the interval $S \in (0.001, 0.05)$, which is roughly consistent with findings in [32]. For $S \leqslant 0.001$ the slope is Poissonian, as $P(S = 0) \neq 0$.

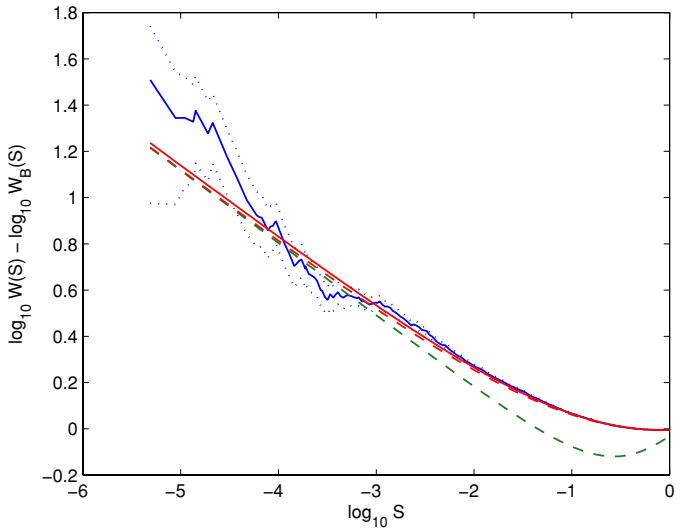

Figure 6. $\log W(S) - \log W_{\rm B}(S)$ versus $\log S$ for $\lambda = 0.15$ for the data with the estimated statistical error (dotted). Here $W_{\rm B}(S)$ is the best fitting Brody distribution with $\beta = 0.313$ over the interval $0.001 \leqslant S \leqslant 1$. The full curve is 2D TBRB analytic theory with the the quantal $\rho_1 = 0.183$ and it captures the numerical data perfectly down to at least $S = 10^{-3}$, with parameter values $\beta = 0.465$ and $\sigma = 0$, and the dashed line close to it is for classical $\rho_1 = 0.175$. The two curves almost overlap. The other dashed curve deviating more strongly from the full line is just BR for comparison.

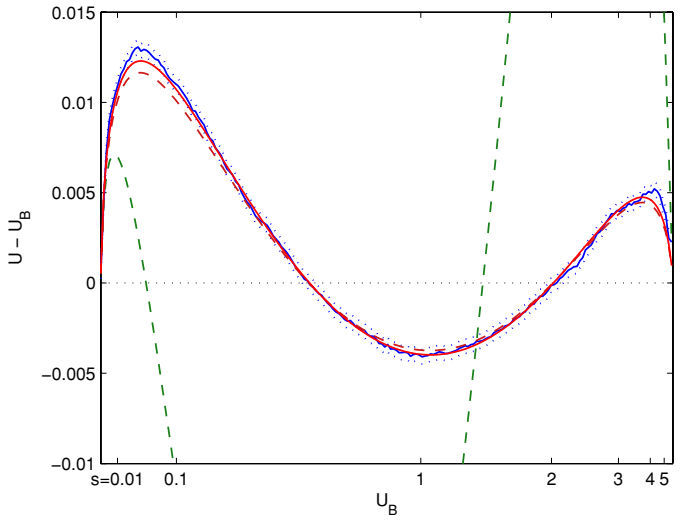

Figure 7. U-function plot (with the expected $\pm$ statistical error) for $\lambda = 0.15$. The full curve is the analytic theory TBRB with $\rho_1 = 0.183$, $\beta = 0.465$ and $\sigma = 0$. The classical value of ρ_1 is 0.175 and the corresponding curve is the dashed one close to the full line, whilst the other dashed curve is just BR.

Finally, at the finest scale, in figure 7 we plot the U-function in the same style as in figure 1, and for the same data as in figure 5, and see almost perfect agreement between the

numerics and the TBRB theory with the above stated parameter values. We see great deviation from the best BR curve (dashed), and also from the Brody curve (the abscissa), thus confirming that the fractional power law level repulsion breaks down at the smallest spacings S. We also see that the tunneling couplings are very small, in fact negligible, so that $\sigma = 0.001$ yields the same result within the graphical resolution like $\sigma = 0$. Please observe that the perfect agreement extends over the entire range of $S \approx 0.003$ up to $S > 5$.

The physical interpretation of these results is clear. We have divided classical phase space with $\rho_1 = 0.175$, the chaotic eigenstates (their Wigner functions) are quite strongly localized with the Brody parameter $\beta = 0.465$, and the regular and chaotic states are only very weakly, or even negligibly, coupled due to the tunneling effects. We have taken into account the energy levels in the range $k = \sqrt{E} \in [2000, 3000]$. The statistical significance is very high, as we have $N_s = 650\,000$ objects in the histograms, and the expected statistical fluctuations are small as indicated by the plus–minus one standard deviation strip in the U-function plot. We claim that this agreement and success of our approach is certainly not accidental, although the other cases at different shape parameters λ do not show such perfect agreement, as we shall discuss below. A closer inspection of the Wigner functions of eigenstates qualitatively confirms this picture, but the quantitative details are subject of a separate paper [44].

We have also used the Izrailev distribution, several versions [22, 25, 26], instead of the Brody distribution for E_c, see equation (8), but found that in the best fit procedure the Brody distribution gave much better agreement of our theory with the numerical spectra.

5. Numerical spectra for other shapes λ and further application of the TBRB theory

We have analyzed the energy spectra of other billiard shapes as well. The general comment is that the tunneling effects and σ are very small or almost absent, hence $\sigma = 0$, whilst the localization effects are quite strong, leading to the BRB level spacing distribution instead of BR. Quite often, ρ_1 needed to find the best or even perfect agreement between the theory and the numerics is larger than the classical value, thereby also capturing the localization effects in the sense of making the effective regular component larger than in the classical dynamics. Sometimes, on rare occasions, the quantal value of ρ_1 is less than the classical ρ_1. In order to understand in detail why this is so, we have to study the structure of eigenstates and the corresponding Wigner functions in the 'quantum phase space'.

Such a situation is met e.g. in the case of $\lambda = 0.125$. In figure 8 we show the U-function plot with the best fit parameters $\sigma = 0$, $\beta = 0.29$ and $\rho_1 = 0.6$. The classical value of ρ_1 is 0.38. The agreement is practically perfect.

In the case of $\lambda = 0.14$ we again find very good agreement at not too large S, namely up to $S \approx 3$, with the classical $\rho_1 = 0.24$, $\beta = 0.295$ and $\sigma = 0$. See figure 9.

The next case is $\lambda = 0.16$, figure 10. The agreement is again very good. The theoretical curve (best fit in β, and quantal $\rho_1 = 0.09$) captures the qualitative behavior of numerical spectra, and is expected to improve at higher energies, but still below the BR regime. For this to demonstrate, better numerical methods and computers are needed. Here the quantal $\rho_1 = 0.09$ is smaller than classical $\rho_1 = 0.121$.

In the case $\lambda = 0.175$ (figure 11) again we find practically perfect agreement, if we replace the classical value of $\rho_1 = 0.05$ with the best fit value $\rho_1 = 0.061$ and take $\beta = 0.718$. Here again the quantal effective ρ_1 is larger than the classical one, capturing the fact that the localized chaotic eigenstates occupy less volume than the classical chaotic component. In other words, the effective quantal regular component is larger than the classical one.

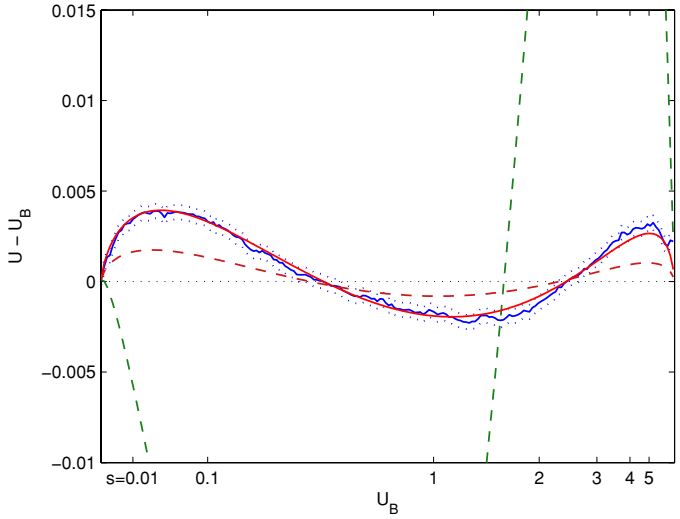

Figure 8. U-function plot (the data with $\pm$ expected statistical error) for $\lambda = 0.125$ with the best fit parameters $\sigma = 0$, $\beta = 0.29$ and quantal $\rho_1 = 0.6$ (full line) and the classical value of $\rho_1 = 0.38$ (the inner dashed line), whilst the outer dashed curve is just BR. $k = \sqrt{E} \in [2000, 3000]$, $N_s = 640\,000$.

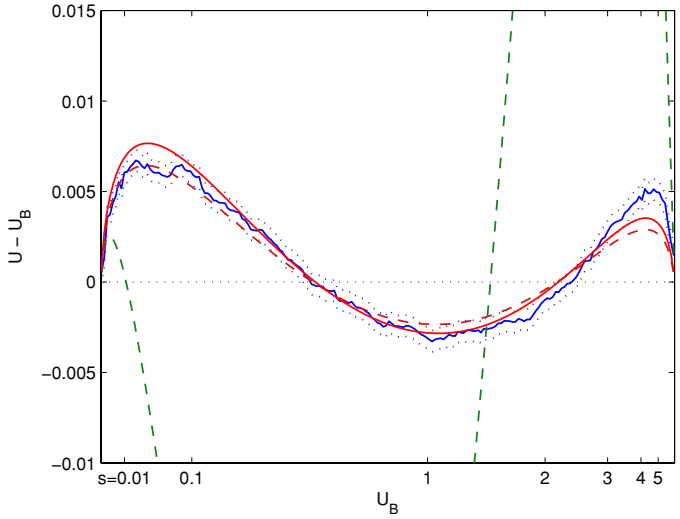

Figure 9. U-function plot (the data with $\pm$ expected statistical error) for $\lambda = 0.14$ with the best fit parameters $\sigma = 0$, $\beta = 0.295$ and quantal $\rho_1 = 0.27$ (full line) and the classical $\rho_1 = 0.24$ (dashed close to the data). The outer dashed line is just BR. $k = \sqrt{E} \in [2000, 2500]$, $N_s = 300\,000$.

In the almost fully chaotic (but not yet strictly ergodic) case[1] at $\lambda = 0.20$, shown in figure 12 we find $\rho_1 = 0$, $\sigma = 0$ and $\beta = 0.67$, thus exhibiting a pure Brody distribution, far

[1] There are thin whispering gallery regions (of Lazutkin) bounded by invariant tori, as the billiard boundary is analytic and convex, and also very small regular islands near the stable periodic orbits.

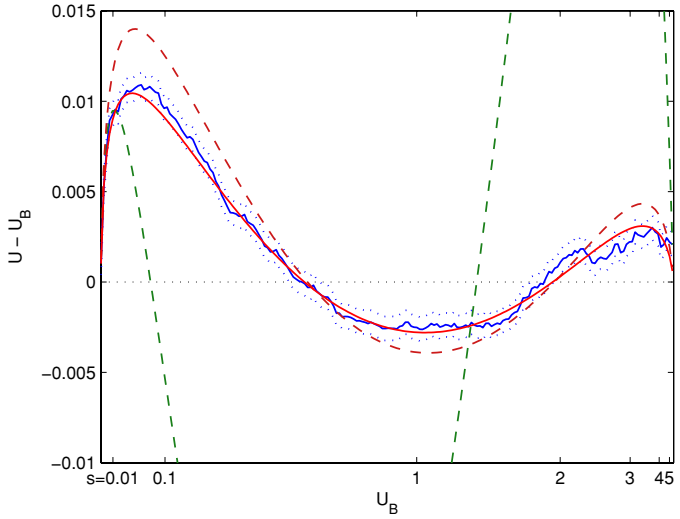

Figure 10. U-function plot (the data with $\pm$ expected statistical error) for $\lambda = 0.16$ with the best fit parameters $\sigma = 0$, $\beta = 0.446$ and quantal $\rho_1 = 0.09$ (the full line) and the classical $\rho_1 = 0.121$ (the inner dashed line). The outer dashed line is just BR. $k = \sqrt{E} \in [2000, 2400]$, $N_s \approx 300\,000$.

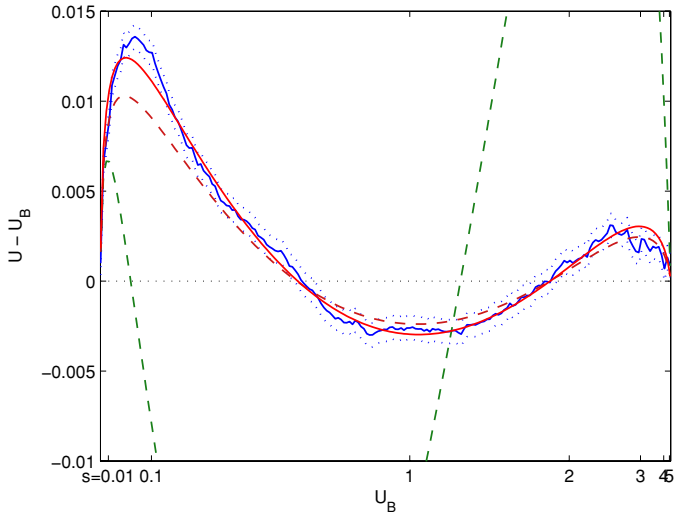

Figure 11. U-function plot (the data with $\pm$ expected statistical error) for $\lambda = 0.175$ with the best fit parameters $\sigma = 0$, $\beta = 0.718$ and the quantal $\rho_1 = 0.061$ (full line), and with classical $\rho_1 = 0.05$ (the inner dashed line). $k = \sqrt{E} \in [2000, 2400]$, $N_s \approx 300\,000$. The outer dashed line is just BR.

away from GOE, implying that the chaotic eigenstates here are still strongly localized (in the mean).

Similarly, in the almost fully chaotic (but not yet strictly ergodic[2]) case at $\lambda = 0.25$, shown in figure 13 we find $\rho_1 = 0$, $\sigma = 0$ and $\beta = 0.89$, thus exhibiting a pure Brody distribution,

[2] Here the boundary has a zero curvature point at $\phi = \pi$ or $z = -1$ or $w = -3/4$, and therefore due to the Mather theorem the whispering gallery modes (of Lazutkin) are all broken, but there are nevertheless still very small islands of stability around the stable periodic orbits which still exist.

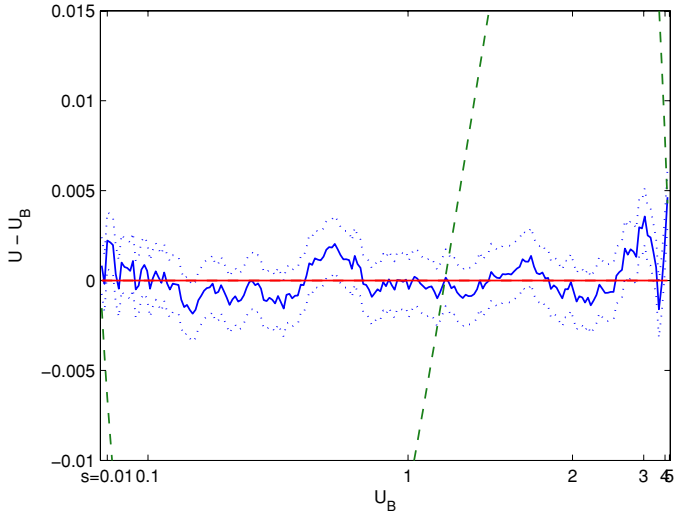

Figure 12. U-function plot for $\lambda = 0.20$ with the best fit parameters $\sigma = 0$, $\beta = 0.67$ and the quantal and classical $\rho_1 = 0.0$. $k = \sqrt{E} \in [0, 550]$, $N_s \approx 40\,800$. Here the level spacing distribution is already purely Brody (the abscissa). The dashed curve is GOE.

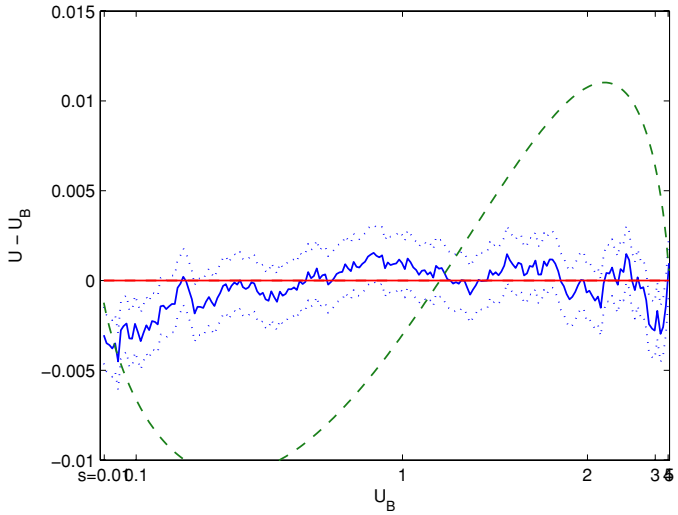

Figure 13. U-function plot for $\lambda = 0.25$ with the best fit parameters $\sigma = 0$, $\beta = 0.89$ and the quantal and classical $\rho_1 = 0.0$, and $k = \sqrt{E} \in [0, 540]$, $N_s \approx 40\,800$. Here the level spacing distribution is already purely Brody (abscissa). The dashed curve is GOE.

still significantly away from GOE, implying that the chaotic eigenstates here are still localized (in the mean), but less strongly than in the case of figure 12, as should be expected.

6. The Prosen billiard and the mushroom billiard

We have also studied the Prosen billiard [28, 29] defined in polar coordinates as $r(\varphi) = 1 + a\cos(4\varphi)$. For $a = 0.04$ the classical $\rho_1 = 0.092$, and we have calculated the energy

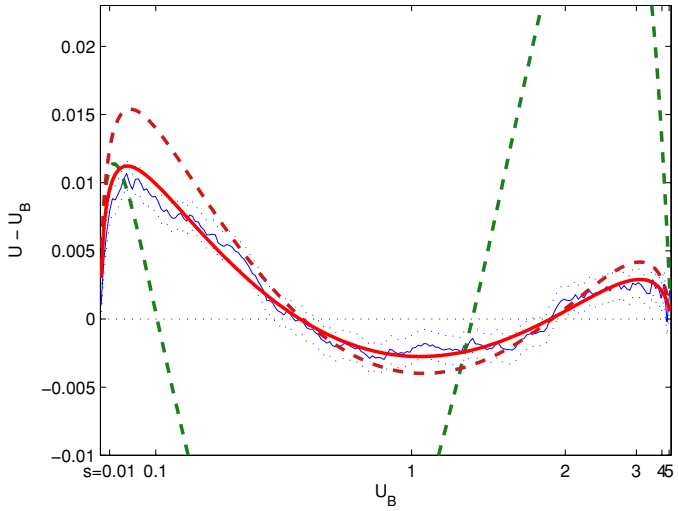

Figure 14. U-function plot for the Prosen billiard $a = 0.04$. The full curve is BRB with quantal $\rho_1 = 0.066$ and $\beta = 0.65$, the dashed curve is BRB with classical $\rho_1 = 0.092$ and $\beta = 0.694$. The outer dashed curve is just BR with the classical ρ_1. The spectral stretch includes levels from 5000–100 000.

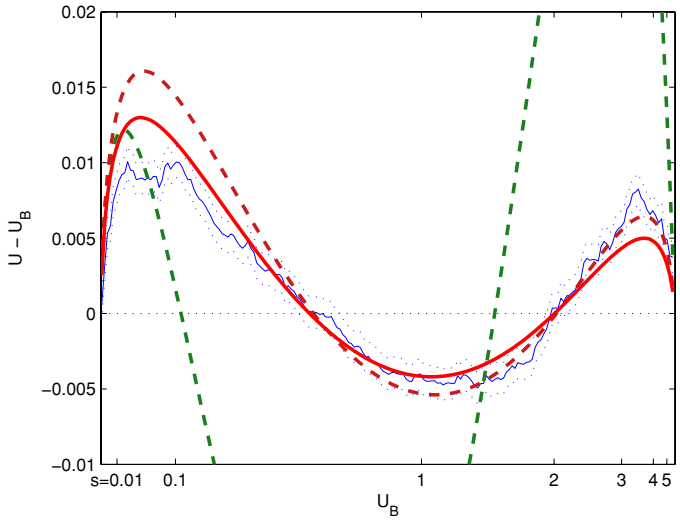

Figure 15. U-function plot for the Prosen billiard $a = 0.03$. The full curve is BRB with quantal $\rho_1 = 0.18$ and $\beta = 0.5$, the dashed curve is BRB with classical $\rho_1 = 0.218$ and $\beta = 0.557$. The outer dashed curve is just BR with the classical ρ_1. The spectral stretch includes levels from 5000–100 000.

spectrum for the low-lying levels with sequential number 5×10^3–1×10^5, using the scaling method of Vergini and Saraceno, based on plane waves. The results are shown in figure 14. We see that the effects of tunneling are completely absent and BRB model applies.

We did the same thing for another value of $a = 0.03$. The classical $\rho_1 = 0.218$. The results are shown in figure 15. We again see that the effects of tunneling are completely absent and BRB model applies.

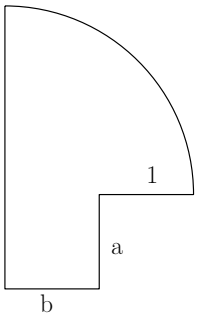

Figure 16. The geometry of the mushroom billiard introduced by Bunimovich [27].

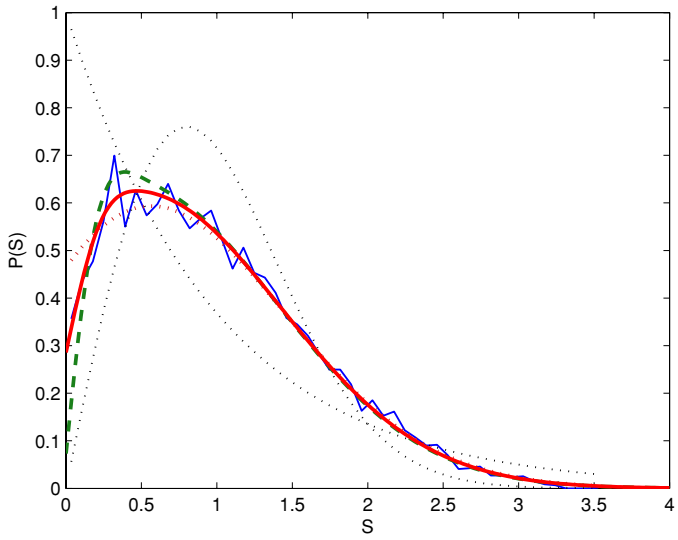

Figure 17. $P(S)$ for the mushroom billiard with the energy spectrum exactly as in [20]. The full curve is TBRB with classical $\rho_1 = 0.268$, $\beta = 1$ and $\sigma = 0.1$. The dashed curve is TDBR with the same parameters, and the thick dotted curve is just BRB ($\sigma = 0$) and the same $\beta = 1$ and ρ_1. The thin dotted curves are just Poisson and GOE.

We have also investigated the so-called mushroom billiard introduced by Bunimovich [27] for the geometrical configuration as shown in figure 16. It has the important property that there is exactly one chaotic component and exactly one regular component in the classical phase space. Moreover, it exhibits 'fast ergodicity', and therefore we do not expect strong dynamical localization effects.

The aim is to demonstrate the effects of tunneling, as has been done in [20], which can be expected only at very low-lying eigenstates, due to the exponential dependence on $1/\hbar_{\mathrm{eff}}$. Therefore, we have taken exactly the same spectra as in [20] (figure 8) and analyzed them in the light of the present TBRB theory. While in [20] the agreement with the TDBR has been found at spacings about $S \geqslant 0.1$, here we find deviation from that model at smaller spacings, but in excellent agreement with the present TBRB theory, as shown in figure 17 for $P(S)$ and in figure 18 for the U-function plot. It is found that $\beta = 1$, thus there is no

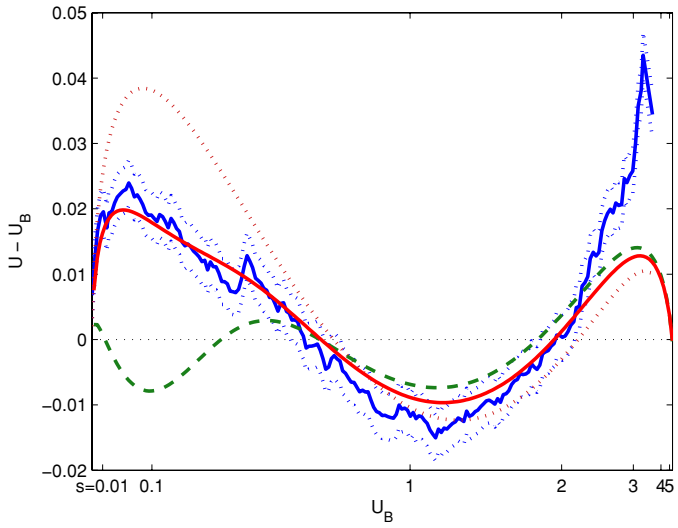

Figure 18. U-function plot for the mushroom billiard with the energy spectrum exactly as in Vidmar *et al* [20]. The full curve is TBRB with classical $\rho_1 = 0.268$, $\beta = 1$ and $\sigma = 0.1$. The dashed curve is TDBR with the same parameters, and the dotted curve is just BRB ($\sigma = 0$) with the same $\beta = 1$ and ρ_1. We see that the TBRB coupling model is much better than TDBR, especially at small spacings.

localization present, whilst the classical $\rho_1 = 0.268$ and $\sigma = 0.1$ give excellent description of the numerical spectra. The discrepancy between the data and the theory at $S \geqslant 2.5$ is due to the statistical errors (not enough independent objects in the sample).

7. Discussion and conclusions

In this paper we have shown that below the asymptotic BR regime (the deep semiclassical limit of sufficiently small effective Planck constant) we find the quasi-universal regime where the effects of the dynamical localization of chaotic eigenstates (in the phase space, as described by the Wigner functions) and the effects of couplings due to tunneling between the regular and chaotic eigenstates can be *on the average* modeled by the new semiempirical TBRB theory with three parameters: ρ_1 which is the relative Liouville volume of the regular components in the classical phase space, the Brody parameter β describing the degree of localization, and the σ parameter describing the strength of the tunneling couplings.

We have introduced as a model the ensemble of large matrices with a Poissonian diagonal block of relative size ρ_1, the chaotic (but localized) diagonal block of relative size $\rho_2 = 1 - \rho_1$ with the Brody distribution having a parameter β, and the off-diagonal coupling elements (uniform random coupling of all states, regular and chaotic), with the sparsity parameter $s = 2\rho_1(1 - \rho_1)$, and with variance σ^2, usually taken to be Gaussian, although other distributions like exponential have been tested as well, and it is found that the results depend only weakly on the kind of distribution functions, especially at not too large σ, as long as they have the same variance σ^2.

We have developed an analytic theory which improves and generalizes the theory in a recent paper by Vidmar *et al* [20] by introducing the localization effects. The theory is still based on an effective two-level model, capturing all the essential features of the large random

matrix ensembles described above (sparsed couplings), rather than the block matrices from [20]. In appendix C we summarize the three different random matrix coupling models.

This analytic theory (TBRB) has been tested in the case of a mixed-type dynamical system, namely the billiard introduced by Robnik [34, 35], and largely perfect agreement has been found. In cases of not so perfect agreement we have reasons to believe that— apart from the possible statistical fluctuations—we are still not in the sufficiently deep semiclassical limit, and that the localization effects cannot yet be entirely described on the average by one parameter β, which is expected to occur at higher energies. The reason really is that at such lower energies and the given classical dynamics other types of localization play an important role, e.g. the effects of sticky objects in the classical phase space, like cantori. See the excellent review by Prosen [21]. Nevertheless, the important conclusion is that the dynamical localization is typically a very strong dominating effect which persists even to such high-lying states like one million above the ground state. On the other hand, the tunneling effects typically disappear very quickly with increasing energy, due to the exponential dependence on the reciprocal effective Planck constant $1/\hbar_{\mathrm{eff}}$. This has been reconfirmed also in the Prosen billiard, for two geometries, $a = 0.04$ and 0.03.

In the so-called mushroom billiard introduced by Bunimovich [27], also studied in this paper, following [20], the classical dynamics is strongly chaotic and the geometry of the (exactly one) chaotic component and its boundary is quite smooth; there are no important sticky objects in the classical phase space. Therefore, the effects of localization are very weak even at low energies, $\beta = 1$, but the tunneling couplings between the (exactly one) regular and the (exactly one) chaotic component are important.

The theory should be tested in other billiards or dynamical systems, for example in the hydrogen atom in the strong magnetic field [39–43, 45].

The important open theoretical issues are the understanding of the details of the geometry of quantum eigenstates in the quantum phase space, that is of the Wigner functions, in correspondence with the geometry and structure of the classical phase space and the dynamics (classical diffusion), which will explain why and how the quantal effective ρ_1 deviates from its classical value, and how can be the parameter of dynamical localization β predicted and explained in a semiclassical context.

Acknowledgments

We thank Professor Gregor Veble, University of Nova Gorica, Slovenia, for some help in testing our numerical spectra. This work was supported by the Slovenian Research Agency, the Ministry of Higher Education, Science and Technology of the Republic of Slovenia.

Appendix A.

First we estimate the expected fluctuation (error) of the cumulative (integrated) level spacing distribution $W(S)$, which contains N_s objects. At a certain S we have the probability W that a level is in the interval $[0, W]$ and $1 - W$ that it is in the interval $[W, 1]$. Assuming binomial probability distribution $P(k)$ of having k levels in the first and $N_s - k$ levels in the second interval we have

$$P(k) = \frac{N_s!}{k!(N_s - k)!} W^k (1 - W)^{N_s - k}. \tag{A.1}$$

Then the average values are equal to

$$\langle k \rangle = N_s W, \qquad \langle k^2 \rangle = N_s W + N_s(N_s - 1)W^2, \tag{A.2}$$

and the variance $V(k) = \langle k^2 \rangle - \langle k \rangle^2$,

$$V(k) = N_s W(1 - W). \tag{A.3}$$

But the probability W is estimated in the mean as k/N_s. Its variance is

$$V(W) = V\left(\frac{k}{N_s}\right) = \frac{1}{N_s^2} V(k) = \frac{W(1-W)}{N_s}, \tag{A.4}$$

and therefore the estimated error of W (standard deviation, the square root of the variance) is given by

$$\delta W = \sqrt{V(W)} = \sqrt{\frac{W(1-W)}{N_s}}. \tag{A.5}$$

Transforming now from $W(S)$ to

$$U(S) = \frac{2}{\pi} \arccos \sqrt{1 - W(S)}, \tag{A.6}$$

we show in a straightforward manner that

$$\delta U = \frac{1}{\pi \sqrt{N_s}}, \tag{A.7}$$

and is indeed independent of S. From the (choice of the constant prefactor in the) definition (A.6) one sees that both $U(S)$ and $W(S)$ go from 0 to 1 as S goes from 0 to infinity.

Appendix B.

We briefly describe the numerical method of calculating the relative Liouville (phase space) volume of the chaotic component $\rho_2 = 1 - \rho_1$ in classical Hamilton systems like billiards, which is based on [36], and known under the name *'counting the black cells'*. The relative Liouville volume is certainly not equal the relative area (of the chaotic component) on the SOS, but can be obtained through the relationship found by Meyer [47] for the integrals of any classical function (of coordinates $\mathbf{q}$ and momenta $\mathbf{p}$) $f = f(\mathbf{q}, \mathbf{p})$ over the energy surface E and SOS as follows:

$$\int_{\mathrm{M}} f(\mathbf{q}, \mathbf{p}) \delta(E - H(\mathbf{q}, \mathbf{p}))\, \mathrm{d}\mathbf{q}\, \mathrm{d}\mathbf{p} = \int_{\mathrm{SOS}} f(q, p) \tau(q, p)\, \mathrm{d}q\, \mathrm{d}p, \tag{B.1}$$

where $\delta(x)$ is the Dirac delta function, and $\tau(q, p)$ is the *average* physical return time of a trajectory through the point (q, p) on/from SOS back to SOS, and is formally a constant of motion on the invariant component (either torus or chaotic component). M denotes the entire phase space in which the energy surface $E = H(\mathbf{q}, \mathbf{p})$ is embedded. If we take $f = 1$ we get the phase space volume Φ of the entire energy surface. If we take for f just the characteristic function of the chaotic component denoted by C, $f = \chi_{\mathrm{ch}}$, having the value 1 on C and zero elsewhere, we get the Liouville phase space volume of the chaotic component Φ_{ch}.[3] The quantity ρ_2 is then equal to

$$\rho_2 = \frac{\Phi_{\mathrm{ch}}}{\Phi} = \frac{\int_{\mathrm{C}} \tau\, \mathrm{d}q\, \mathrm{d}p}{\int_{\mathrm{SOS}} \tau\, \mathrm{d}q\, \mathrm{d}p}. \tag{B.2}$$

The idea of the method is first to cover the SOS with a grid of size $N \times N$ small square cells, such that the area of each cell is ϵ. Then an orbit is started in the chaotic region C, and for each

[3] which, according to (B.1), is the integral of τ over C on SOS, and since τ is constant over the entire chaotic component C, Φ_{ch} is formally equal to the product of τ and the area A_{ch} of the chaotic component on the SOS. However, in practice, due to 'slow ergodicity', it is better to proceed as in equations (B.2)–(B.4).

Table B1. We compare the exact and the numerical values of $\rho_1 = 1 - \rho_2$ for some representative parameter values a and b of the mushroom billiard defined in figure 16. The agreement is excellent.

a	b	ρ_{exact}	ρ_{measured}
0.5	0.5	0.511 255	0.5110
1	1	0.296 594	0.2963
0.5	1	0.337 317	0.3371
0.5	0.25	0.678 000	0.6778

cell with coordinates (i, j) and index $k = k(i, j)$ we then have a counter $\eta(k)$, which increases by 1 on each visit at t (discrete time = number of SOS crossings, in the case of billiards, this is the number of collisions at the boundary), namely

$$\eta(k) \to \eta(k) + 1. \tag{B.3}$$

The second counter is the *phase space volume* $\Phi(k)$ which increases as follows:

$$\Phi(k) \to \Phi(k) + \epsilon\tau(t), \tag{B.4}$$

where $\tau(t)$ is the real physical return time of the actual physical orbit from SOS to SOS, on $(t - 1) \to t$. At the end of calculation we replace $\Phi(k)$ by $\Phi(k)/\eta(k)$ and sum up all $\Phi(k)$, to get Φ_{ch}. If we do the same thing for the entire SOS, starting a trajectory in each cell, we get Φ. Formula (B.2) then gives ρ_2. In our calculations we have typically taken $N = 5000$.

The method has been very carefully tested, like in the unpublished works of Dobnikar [48] and Vidmar [49]. The most rigorous test is by comparing the numerical results with the analytical results. For the mushroom billiard as defined in figure 16 there exists an exact analytic formula [46] for $\rho_2 = 1 - \rho_1$, namely

$$\rho_2 = \mathcal{B}/\mathcal{A}, \tag{B.5}$$

where $\mathcal{A} = ab + \frac{\pi}{4}(b + 1)^2$ is the area of the billiard and

$$\mathcal{B} = ab + \frac{1}{2}\left((b + 1)^2 \arcsin\left(\frac{b}{b + 1}\right) + b\sqrt{1 + 2b}\right). \tag{B.6}$$

In table B1 we compare the results on $\rho_1 = 1 - \rho_2$ for some representative values of a and b. The agreement is excellent.

Another test of accuracy was the diamond billiard, which is ergodic, and we indeed obtained numerically $\rho_2 = 1 - \rho_1 = 0.9997$.

Appendix C.

Here we summarize the definitions and properties of the three $N \times N$ random real symmetric matrix coupling models, as shown in figure C1 and the corresponding two-level analytical theory for the level spacing distribution $P(S)$. In all three cases we have on the diagonal a Poisson block of size $\rho_1 N$ and a Brody block with parameter β and of size $\rho_2 N$, where $\rho_2 = 1 - \rho_1$. Thus, the level spacing distribution of the diagonal elements is BRB (Berry–Robnik–Brody) for all three models, i.e. $P_{\text{BRB}}(S)$. The differences appear in the structure of the off-diagonal coupling terms. All non-zero off-diagonal matrix elements b have the same Gaussian distribution (14).

A-model. All off-diagonal matrix elements are non-zero; thus, we have all-to-all couplings, such as those that appear e.g. due to a global perturbation in the system, for example in the

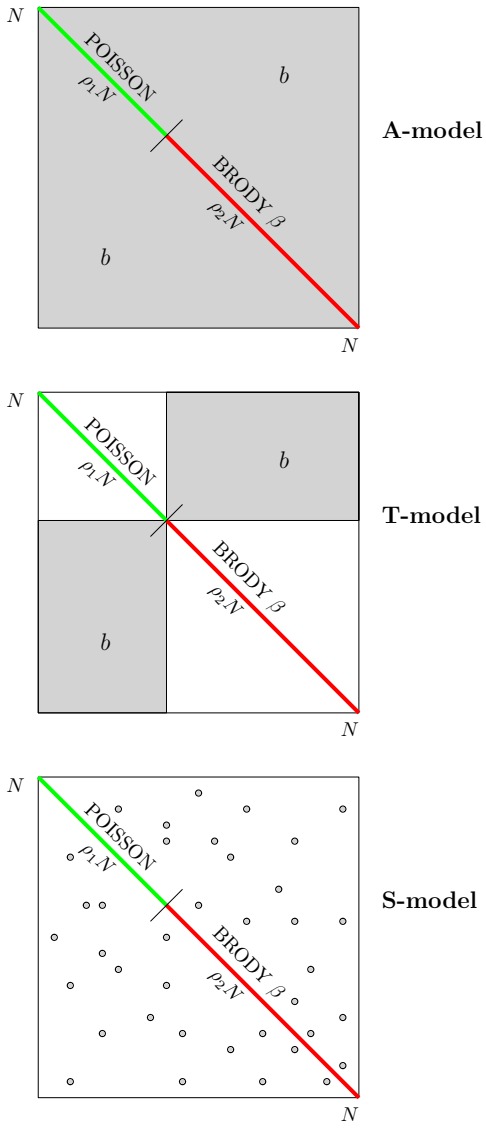

Figure C1. The structure of the three different coupling models in the form of large $N\times N$ random matrices.

microwave resonators due to the existence of an antenna inside the cavity. In [20] the model was termed ADBR (antenna-distorted Berry–Robnik), but now is generalized to include the localization effects. The theoretical two-level level spacing distribution is obtained by using directly the coupling formula (11), and is given by

$$P(S) = \frac{S}{\sigma\sqrt{2\pi}} \int_0^{\pi/2} P_{\mathrm{BRB}}(S\cos\varphi) \exp\left(-\frac{(S\sin\varphi)^2}{8\sigma^2}\right) \mathrm{d}\varphi. \tag{C.1}$$

T-model. Here only the regular (r) and chaotic (c) levels are coupled; therefore, the non-zero off-diagonal elements reside only within the off-diagonal blocks as indicated in figure C1. The theoretical two-level level spacing distribution $P(S)$ is given by equation (20), namely

$$P(S) = P_{\mathrm{rr}}(S) + P_{\mathrm{cc}}(S) + \frac{S}{\sigma\sqrt{2\pi}} \int_0^{\pi/2} P_{\mathrm{rc}}(S\cos\varphi) \exp\left(-\frac{(S\sin\varphi)^2}{8\sigma^2}\right) \mathrm{d}\varphi. \tag{C.2}$$

where $P_{\mathrm{rr}}(S)$, $P_{\mathrm{cc}}(S)$ and $P_{\mathrm{rc}}(S)$ are defined in equation (19). Thus, equation (C.2) gives much better theoretical description of the underlying matrix ensemble (generalized TDBR) than the one proposed in [20], especially at small spacings S.

S-model. Here not all off-diagonal elements are non-zero, but only a relative fraction $s = 2\rho_1\rho_2 = 2\rho_1(1-\rho_1)$ of them, which otherwise are uniformly randomly distributed over the off-diagonal matrix elements positions. This is due to the fact that we do not know and assume any specific information on the basis functions, except that they can be classified as regular and/or chaotic. The corresponding level spacing distribution is given by formula (22), namely

$$P(S) = \frac{2\rho_1(1-\rho_1)S}{\sigma\sqrt{2\pi}} \int_0^{\pi/2} P_{\mathrm{BRB}}(S\cos\varphi) \exp\left(-\frac{(S\sin\varphi)^2}{8\sigma^2}\right) \mathrm{d}\varphi + (1 - 2\rho_1(1-\rho_1))\, P_{\mathrm{BRB}}(S). \tag{C.3}$$

It turns out that the S-model, which is precisely the TBRB model and theory, successfully describes the couplings due to the tunneling in real dynamical systems, much better than the T-model, especially at small spacings S.

References

[1] Stöckmann H-J 1999 *Quantum Chaos—An Introduction* (Cambridge: Cambridge University Press)
[2] Haake F 2001 *Quantum Signatures of Chaos* (Berlin: Springer)
[3] Robnik M 1998 *Nonlinear Phenom. Complex Syst.* **1** 1–22
[4] Mehta M L 1991 *Random Matrices* (Boston, MA: Academic)
[5] Guhr T, Müller-Groeling A and Weidenmüller H A 1998 *Phys. Rep.* **299** 189–428
[6] Robnik M and Berry M V 1986 *J. Phys. A: Math. Gen.* **19** 669
[7] Robnik M 1986 *Lecture Notes Physics* **263** 120–13
[8] Bohigas O, Giannoni M-J and Schmit C 1984 *Phys. Rev. Lett.* **52** 1
[9] Casati G, Valz-Gris F and Guarneri I 1980 *Lett. Nuovo Cimento* **28** 279
[10] Berry M V 1985 *Proc. R. Soc.* A **400** 229
[11] Sieber M and Richter K 2001 *Phys. Scr.* **T90** 128
[12] Müller S, Heusler S, Braun P, Haake F and Altland A 2004 *Phys. Rev. Lett.* **93** 014103
[13] Heusler S, Müller S, Braun P and Haake F 2004 *J. Phys. A: Math. Gen.* **37** L31
[14] Müller S, Heusler S, Braun P, Haake F and Altland A 2005 *Phys. Rev.* E **72** 046207 (arXiv:nlin.CD/0503052v1 23 Mar 2005)
[15] Müller S, Heusler S, Altland A, Braun P and Haake F 2009 *New J. Phys.* **11** 103025 (arXiv:0906.1960v2 [nlin.CD])
[16] Robnik M and Veble G 1998 *J. Phys. A: Math. Gen.* **31** 4669–704
[17] Berry M V and Robnik M 1984 *J. Phys. A: Math. Gen.* **17** 2413
[18] Berry M V 1977 *J Phys. A: Math. Gen.* **12** 2083
[19] Prosen T and Robnik M 1999 *J. Phys. A: Math. Gen.* **32** 1863
[20] Vidmar G, Stöckmann H-J, Robnik M, Kuhl U, Höhmann R and Grossmann S 2007 *J. Phys. A: Math. Theor.* **40** 13883
[21] Prosen T 2000 *Proc. Int. School of Physics "Enrico Fermi", Course CXLIII* ed G Casati, I Guarneri and U Smilyanski (Amsterdam: IOS) p 473
[22] Izrailev F M 1990 *Phys. Rep.* **196** 299
[23] Prosen T and Robnik M 1994 *J. Phys. A: Math. Gen.* **27** L459
[24] Prosen T and Robnik M 1994 *J. Phys. A: Math. Gen.* **27** 8059

[25] Izrailev F M 1988 *Phys. Lett.* A **134** 13
[26] Casati G, Izrailev F M and Molinari L 1991 *J. Phys. A: Math. Gen.* **24** 4755
[27] Bunimovich L A 2001 *Chaos* **11** 802
[28] Prosen T 1998 *J. Phys. A: Math. Gen.* **31** L345
[29] Prosen T 1998 *J. Phys. A: Math. Gen.* **31** 7023
[30] Grossmann S and Robnik M 2007 *J. Phys. A: Math. Theor.* **40** 409–21
[31] Grossmann S and Robnik M 2007 *Z. Nat. forsch.* A **62** 471–82
[32] Prosen T and Robnik M 1993 *J. Phys. A: Math. Gen.* **26** 2371
[33] Prosen T and Robnik M 1993 *J. Phys. A: Math. Gen.* **26** 1105–14
[34] Robnik M 1983 *J. Phys. A: Math. Gen.* **16** 3971
[35] Robnik M 1984 *J. Phys. A: Math. Gen.* **17** 1049
[36] Robnik M, Dobnikar D, Rapisarda A, Prosen T and Petkovšek M 1997 *J. Phys. A: Math. Gen.* **30** L803
[37] Veble G, Prosen T and Robnik M 2007 *New J. Phys.* **9** 15
[38] Vergini E and Saraceno M 1995 *Phys. Rev.* E **52** 2204
[39] Robnik M 1981 *J. Phys. A: Math. Gen.* **14** 3195–216
[40] Robnik M 1982 *J. Phys. Colloq.* C2 **43** 29
[41] Hasegawa H, Robnik M and Wunner G 1989 *Prog. Theor. Phys. Suppl. (Kyoto)* **98** 198–286
[42] Wintgen D and Friedrich H 1989 *Phys. Rep.* **183** 38
[43] Ruder H, Wunner G, Herold H and Geyer F 1994 *Atoms in Strong Magnetic Fields* (Heidelberg: Springer)
[44] Batistić B and Robnik M 2010a (in preparation)
[45] Batistić B and Robnik M 2010b (in preparation)
[46] Bäcker A, Ketzmerick R, Löck S, Robnik M, Vidmar G, Höhmann R, Kuhl U and Stöckmann H-J 2008 *Phys. Rev. Lett.* **100** 174103
[47] Meyer H D 1985 *J. Chem. Phys.* **84** 3147
[48] Dobnikar J 1996 *Diploma Thesis* CAMTP
[49] Vidmar G 2008 *PhD Thesis* CAMTP